Unsteady Ekman-Stokes Dynamics: Implications for Surface Wave-Induced Drift of Floating Marine Litter

Christopher Higgins[1,2], Jake Cunningham[1,3], Jacques Vanneste[4] & Ton van den Bremer[1,5]

1. Department of Engineering Science, University of Oxford.
2. CEA, University Paris-Saclay.
3. Centre for Artificial Intelligence, University College London, UK.
4. School of Mathematics, University of Edinburgh.
5. Faculty of Civil Engineering and Geosciences, TU Delft.

Table of contents

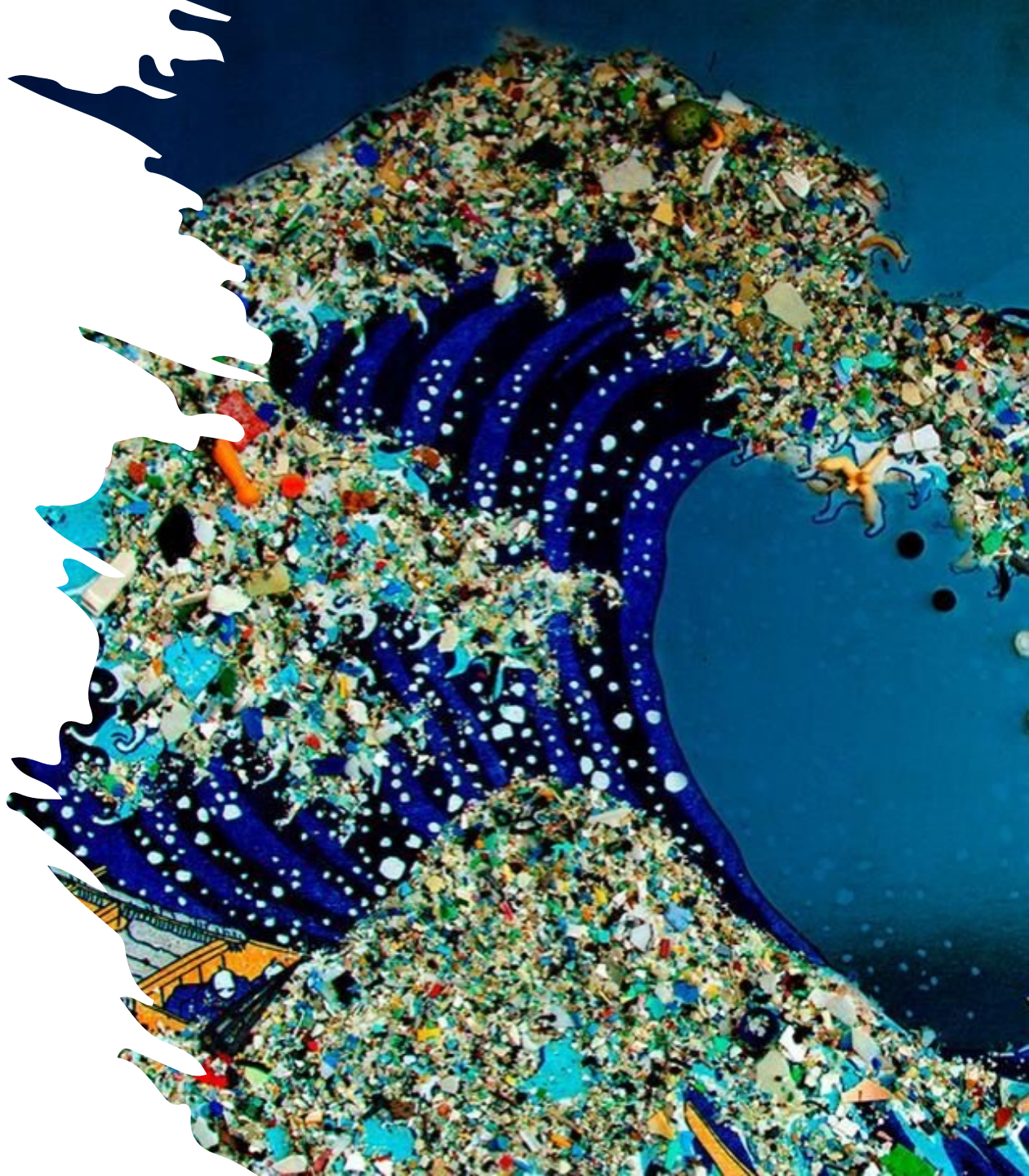

1. Background: wind-driven Ekman dynamics

- Ekman (1905) showed that wind-driven currents at the surface are oriented 45 degrees to the right of wind direction, turning in a decreasing spiral with depth.

- Lewis & Belcher (2004) calculated transient response (diagram on right) to steady wind forcing:

$$\frac{\partial \boldsymbol{U}}{\partial t} + \mathrm{i}f\boldsymbol{U} = \frac{\partial}{\partial z}\left(\nu_{\mathrm{e}}(z)\frac{\partial \boldsymbol{U}}{\partial z}\right)$$

$$\rho\left(\nu_{\mathrm{e}}(z)\frac{\partial \boldsymbol{U}}{\partial z}\right)_{z=0} = \boldsymbol{\tau}_{\mathrm{S}}, \quad \text{at } z = 0$$

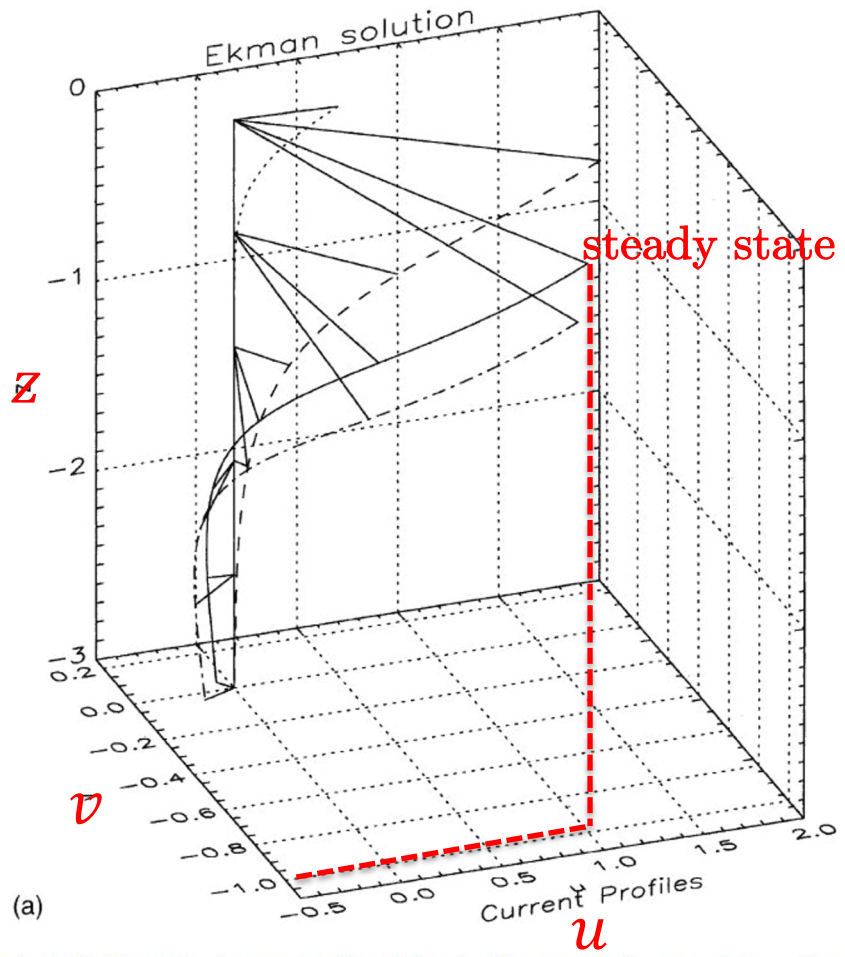

Fig. 2. (a) Evolution of the normalised current profile, $\boldsymbol{U}/U_{\mathrm{C}}$, for the unsteady Ekman solution with non-dimensional time ft. Perspective view of the current profile at: $ft = 0.1$; dashed line: $ft = 1$; dot-dashed line: $ft = 4$; solid line: steady-state profile, $ft \to \infty$.

1. Background: Stokes drift

Lagrangian particle orbit underneath periodic surface gravity wave does not close.

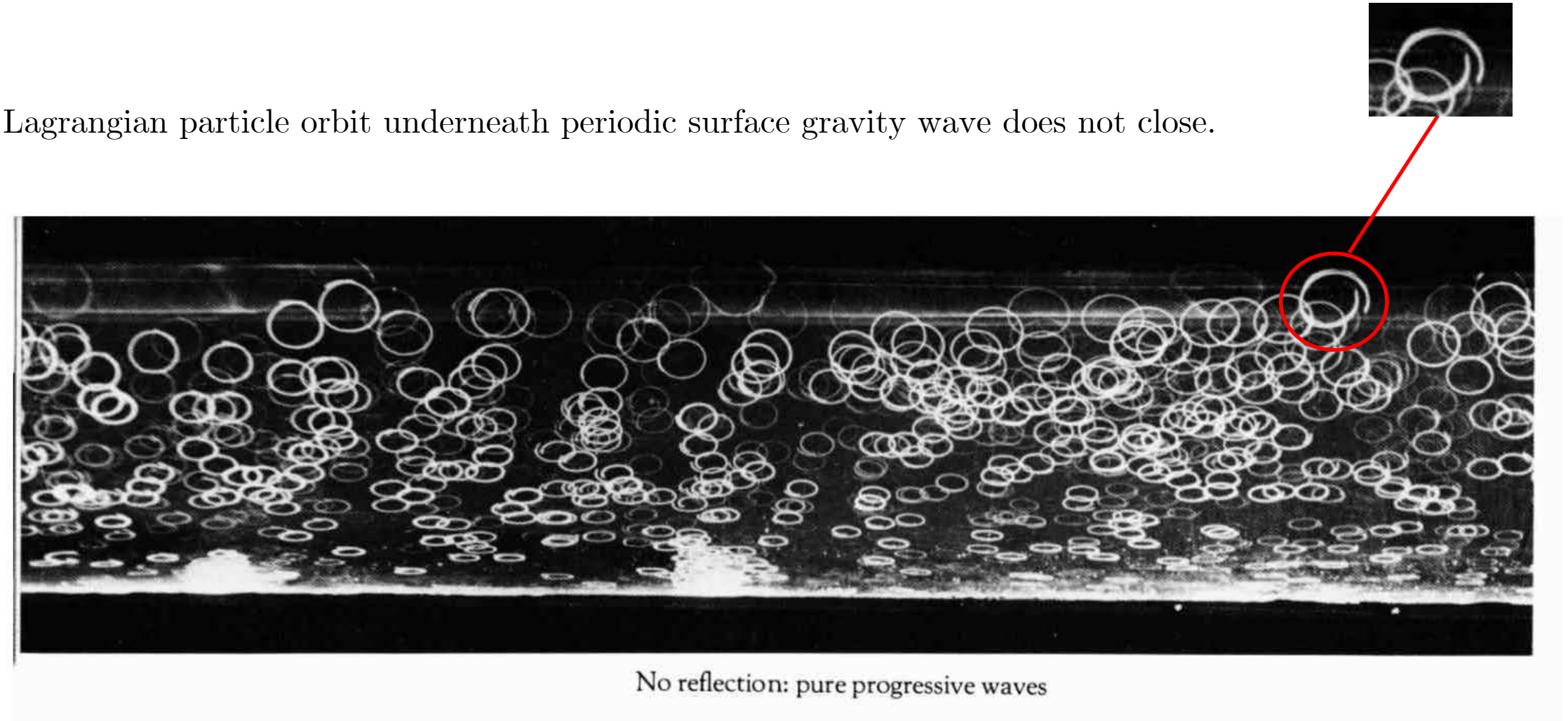

No reflection: pure progressive waves

From Wallet & Ruellan (1950) reproduced in Van Dyke (1982)

1. Background: Stokes drift

- Since particle trajectories are not perfectly closed ellipses, there is a net drift in the wave propagation direction:

$$\frac{d\Delta \boldsymbol{x}_{\mathrm{L}}}{dt} = \boldsymbol{u}(\boldsymbol{x}_0 + \Delta \boldsymbol{x}_{\mathrm{L}}(t), t)$$

- Explicit expression from Stokes expansion:

$$\mathbf{u} = \alpha^1 \mathbf{u}_1 + \alpha^2 \mathbf{u}_2 + \alpha^3 \mathbf{u}_3 + \ldots \qquad \alpha = A_0 k_0$$

$$u_{\mathrm{S}} = \overline{\Delta \boldsymbol{x}_1 \cdot \boldsymbol{\nabla} u_1} = \omega_0 k_0 |A_0|^2 e^{2k_0 z}$$

- Lagrangian = Eulerian + Stokes:

$$\boldsymbol{u}_{\mathrm{L}} = \boldsymbol{u}_2 + \boldsymbol{u}_{\mathrm{S}}$$

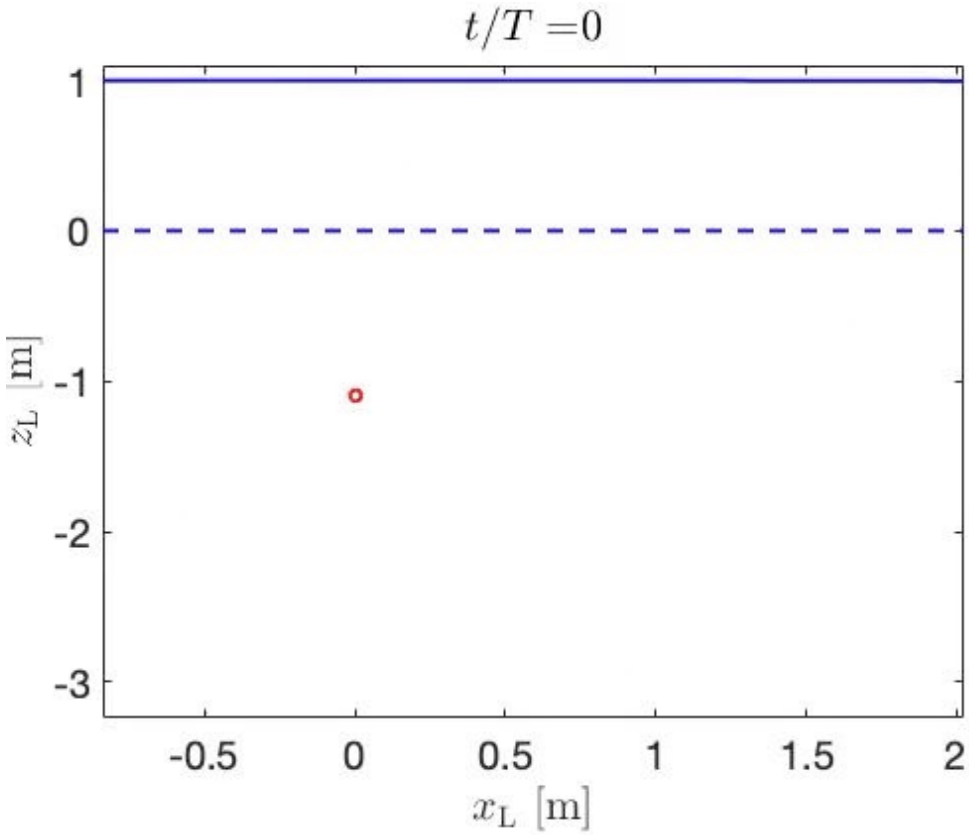

1. Background: Coriolis-Stokes force

- Ursell (1950) shows there can be no net drift for regular waves in a rotating frame: anti-Stokes flow!

- Hasselmann (1970) explains this via a Coriolis-Stokes force on the mean flow:

$$\partial_t \boldsymbol{u}_2 + \boldsymbol{f} \times \boldsymbol{u}_2 + \boldsymbol{\nabla} p_2 = -\boldsymbol{f} \times \boldsymbol{u}_{\mathrm{S}}$$

- Horizontal pressure gradients (and non-traditional Coriolis) are neglected in Hasselmann's calculations.
- For time-dependent Stokes drift:

$$\mathbf{u}_{\pm} = \mathbf{u}_{\pm}(t=0) \mp if \int_0^t \exp\left(\mp if(t-t')\right) u_{\pm}^{\mathrm{st}}(t')\, dt'$$

Sea of undamped inertial oscillations!

2. Ekman-Stokes equations.

- At second order in steepness, the governing equations are:

$$\partial_t \overline{u} - f v_{\mathrm{L}} = -\partial_x \overline{p} + \nu \nabla^2 \overline{u}, \qquad \partial_t \overline{v} + f u_{\mathrm{L}} = -\partial_y \overline{p} + \nu \nabla^2 \overline{v},$$
$$\partial_t \overline{w} = -\partial_z \overline{p} + \nu \nabla^2 \overline{w}, \qquad \partial_x \overline{u} + \partial_y \overline{v} = -\partial_z \overline{w},$$

- After neglecting horizontal derivatives, the Ekman-Stokes equations are:

$$\partial_t \mathcal{U} + i f \mathcal{U} - \nu \partial_z^2 \mathcal{U} = -i f \mathcal{U}_{\mathrm{S}}(x, y, z, t), \quad \partial_z \mathcal{U}|_{z=0} = \partial_z \mathcal{U}_{\mathrm{S}}|_{z=0}, \quad \lim_{z/\delta_{\mathrm{E}} \to -\infty} \mathcal{U} = 0$$

Complex notation: $\boxed{\mathcal{U} = \overline{u} + i\overline{v}}$ $\boxed{\mathcal{U}_{\mathrm{S}} = u_{\mathrm{S}} + i v_{\mathrm{S}}}$

2. Ekman-Stokes equations: wave stress.

- Longuet-Higgins (1953): Surface boundary layer of depth $\delta_\nu = \sqrt{2\nu_{mol}/\omega}$ changes mass transport in the fluid interior beneath.
- Gives rise to 'boundary layer streaming', additional Eulerian transport in the boundary layer.
- Flow is not irrotational close to the surface => vorticity generated => interior flow feels a stress
- Coriolis-Stokes forcing felt over Stokes depth:
- Ekman spiral part of the solution extends over the Ekman depth:

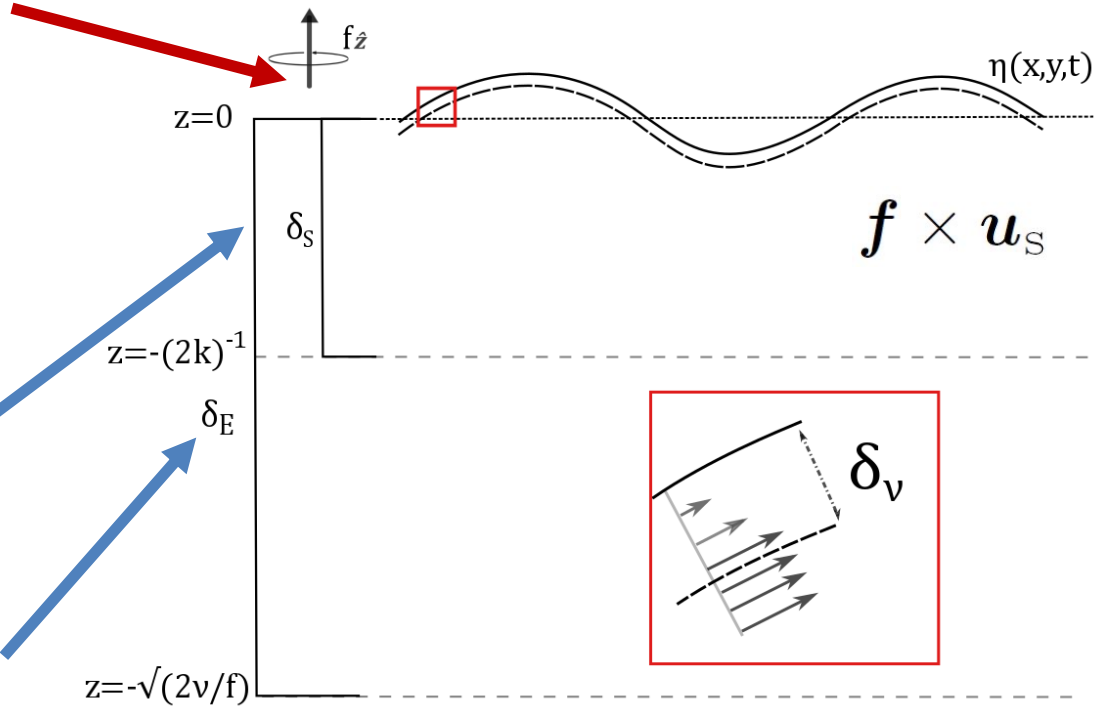

2. Ekman-Stokes flow

- Ekman-Stokes equations (recap):

$$\partial_t \mathcal{U} + if\mathcal{U} - \nu\partial_z^2 \mathcal{U} = -if\mathcal{U}_\mathrm{S}(x,y,z,t), \quad \partial_z \mathcal{U}|_{z=0} = \partial_z \mathcal{U}_\mathrm{S}|_{z=0}, \quad \lim_{z/\delta_\mathrm{E}\to-\infty} \mathcal{U} = 0$$

- The Ekman-Stokes equations can be solved using Laplace transform,

$$\tilde{g}(s) = \mathcal{L}\{g(t)\} = \int_0^\infty g(t)e^{-st}dt$$

$$\tilde{\mathcal{U}} = 2k\left(1 + \frac{if}{s + if - 4k^2\nu}\right)\frac{\tilde{\mathcal{U}}_\mathrm{S} e^{z\sqrt{(s+if)/\nu}}}{\sqrt{(s+if)/\nu}} - \frac{if\tilde{\mathcal{U}}_\mathrm{S} e^{2kz}}{s + if - 4k^2\nu}$$

- Taking s to zero gives the steady-state solution (Seshasayan & Gallet, 2019): $D = \delta_E/\delta_S$

$$\overline{\mathcal{U}} = \frac{(1-i)D}{2}\overline{\mathcal{U}_\mathrm{S}}\left(1 + \frac{1}{1+iD^2/2}\right)e^{(1+i)z/\delta_\mathrm{E}} - \frac{\overline{\mathcal{U}_\mathrm{S}} e^{2kz}}{1+iD^2/2}$$

3. Ekman-Stokes Kernel

- Using Laplace convolution theorem, the Ekman-Stokes flow is given by:

$$\mathcal{U}(\boldsymbol{x}, z, t) = \int_0^t \mathcal{U}_{\mathrm{S}}\left(\boldsymbol{x}, t'\right)|_{z=0} K\left(z\,,\, t - t'\right) dt'$$

- Where the Ekman-Stokes kernel $K(z,t)$ encodes development of flow with depth:

$$K(z,t) = \underbrace{2k\sqrt{\nu}e^{-ift}\frac{e^{-z^2/(4\nu t)}}{\sqrt{\pi t}}}_{\text{Ekman spiral term}} - \underbrace{ife^{\left(4k^2\nu - if\right)t}\sum_{\pm}\frac{e^{\pm 2kz}}{2}\operatorname{erfc}\left(\sqrt{4k^2\nu t} \pm \frac{z}{\sqrt{4\nu t}}\right)}_{\text{Coriolis-Stokes term}}$$

3. Ekman-Stokes Kernel

- When viscosity is neglected (including the molecular viscosity), we recover Hasselmann's result (upon convolution):

$$-ife^{-ift}e^{2kz}$$

- When Coriolis is neglected, we must set $\nu = \nu_{mol}$, leading to Longuet-Higgins' result upon convolution:

$$2k\sqrt{\nu}e^{-z^2/(4\nu t)}/\sqrt{\pi t}$$

Full Ekman-Stokes Kernel (recap):

$$K(z,t) = 2k\sqrt{\nu}e^{-ift}\frac{e^{-z^2/(4\nu t)}}{\sqrt{\pi t}} - ife^{(4k^2\nu - if)t}\sum_{\pm}\frac{e^{\pm 2kz}}{2}\,\mathrm{erfc}\left(\sqrt{4k^2\nu t} \pm \frac{z}{\sqrt{4\nu t}}\right)$$

Decaying inertial oscillation!

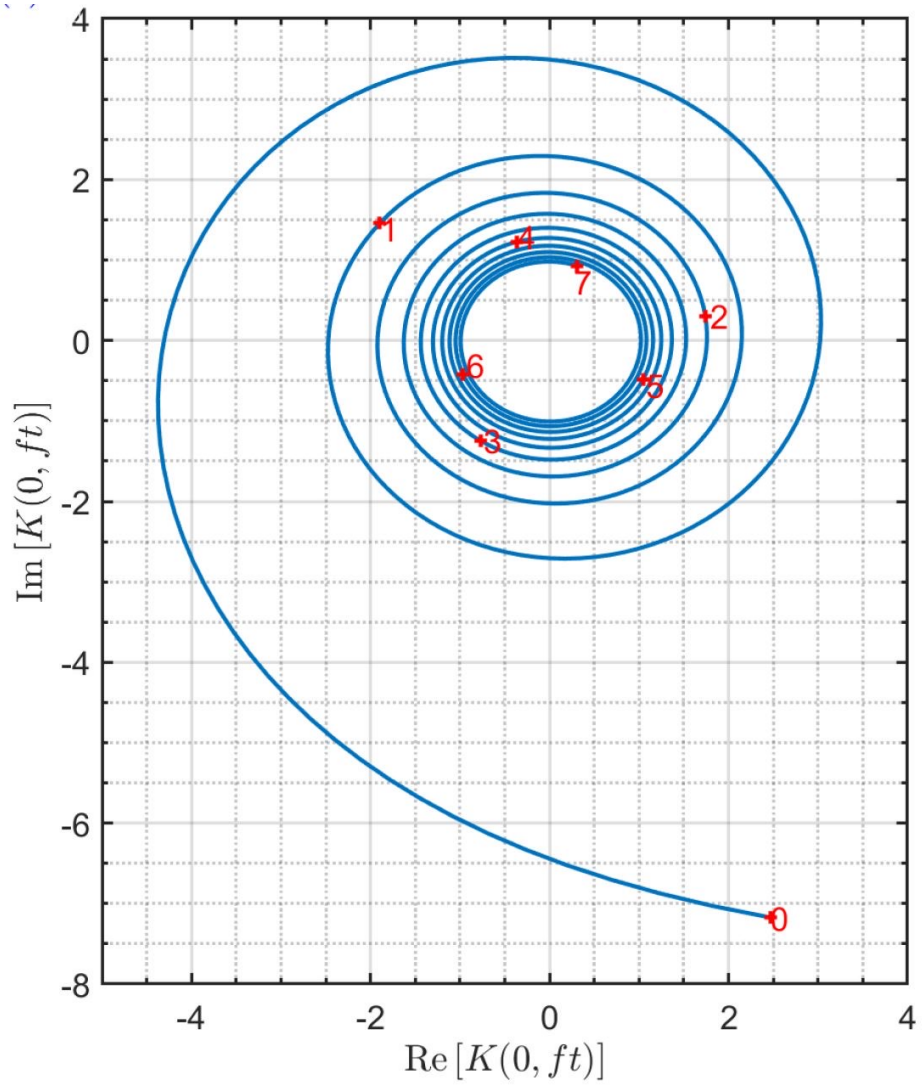

3. Ekman-Stokes Kernel: Gaussian storm

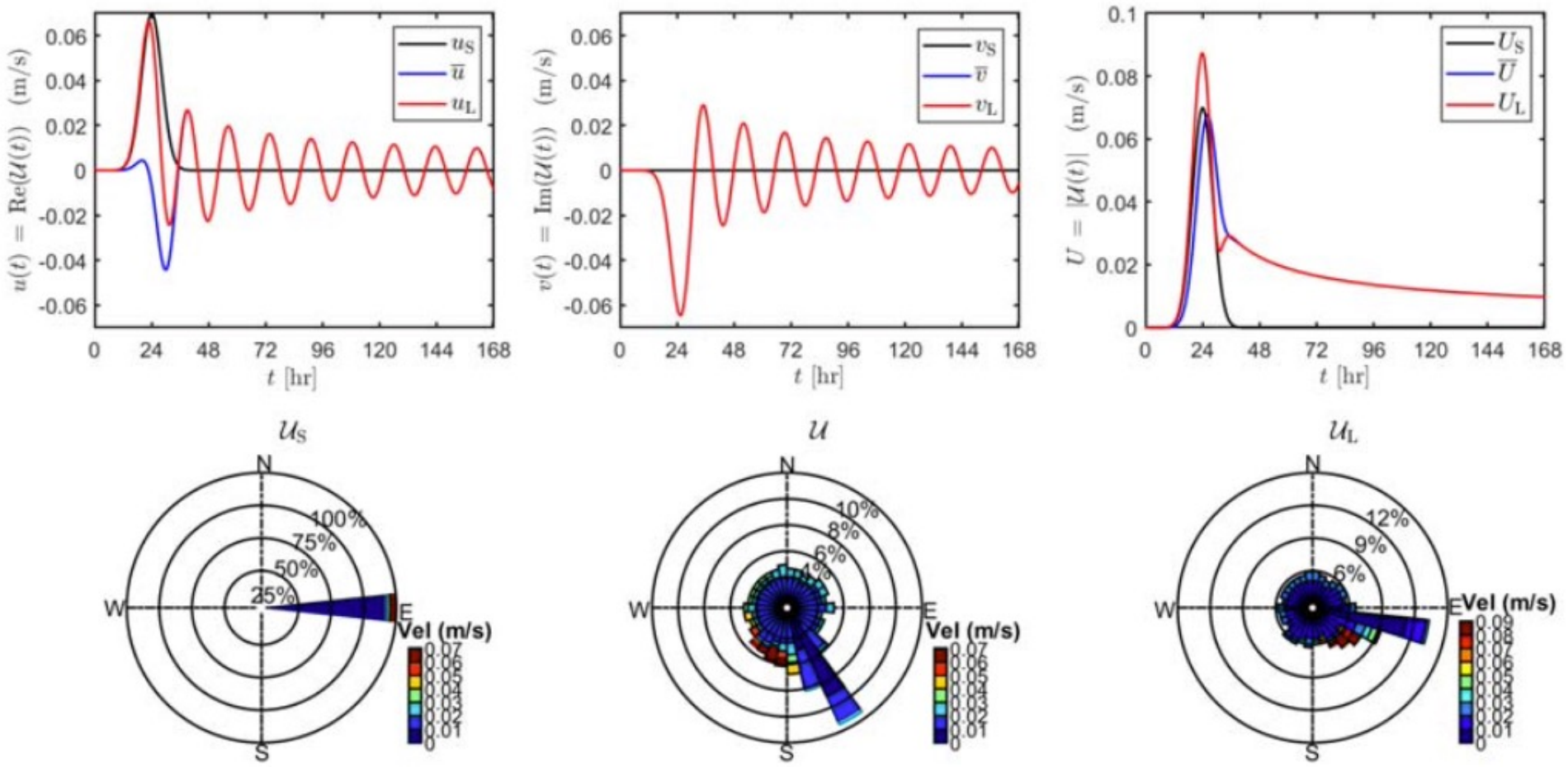

Figure 2. Top: time series of wave-induced velocities formed in response to an idealized 24 hr Gaussian storm in the Northern Hemisphere showing the two components and magnitude of the Stokes drift $\mathcal{U}_S$ (black), Eulerian-mean velocity $\mathcal{U}$ (blue) and Lagrangian velocity $\mathcal{U}_L$ (red). Bottom: wave roses for $\mathcal{U}_S$, $\mathcal{U}$, and $\mathcal{U}_L$, with radial distance representing the fraction of time during which the velocity has a given direction, and color indicating magnitude in m/s.

4. Buoy data

- We obtained data for the San Nicolas Island buoy from CDIP (Coastal Data Information Project)
- We used a monochromatic approximation to find the Stokes drift from buoy data:

$$\mathcal{U}_{\mathrm{S}} = g^{-1}\omega_p^3 A_p^2 \exp(2\overline{k}z)\exp\left(i\theta_p\right)$$

- The Ekman-Stokes convolution is evaluated numerically with δt = buoy sampling time.

$$\mathcal{U}_{\mathrm{n}}(\tau_{\mathrm{n}}) = \sum_{k=0}^{n-1} \mathcal{U}_{\mathrm{S}}(k\delta t) K\left((n-k)\delta t\right)\delta t$$

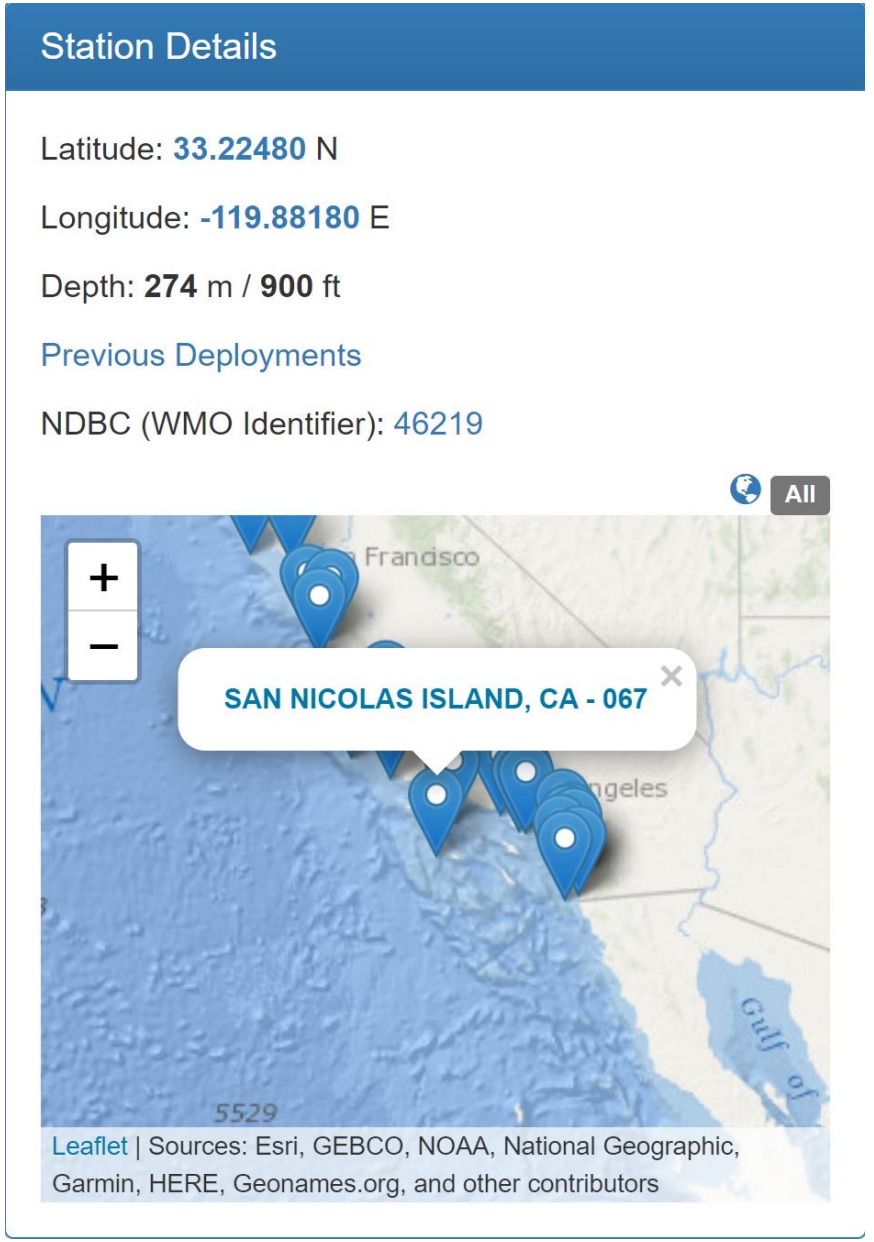

4. Buoy data: Ekman-Stokes flow

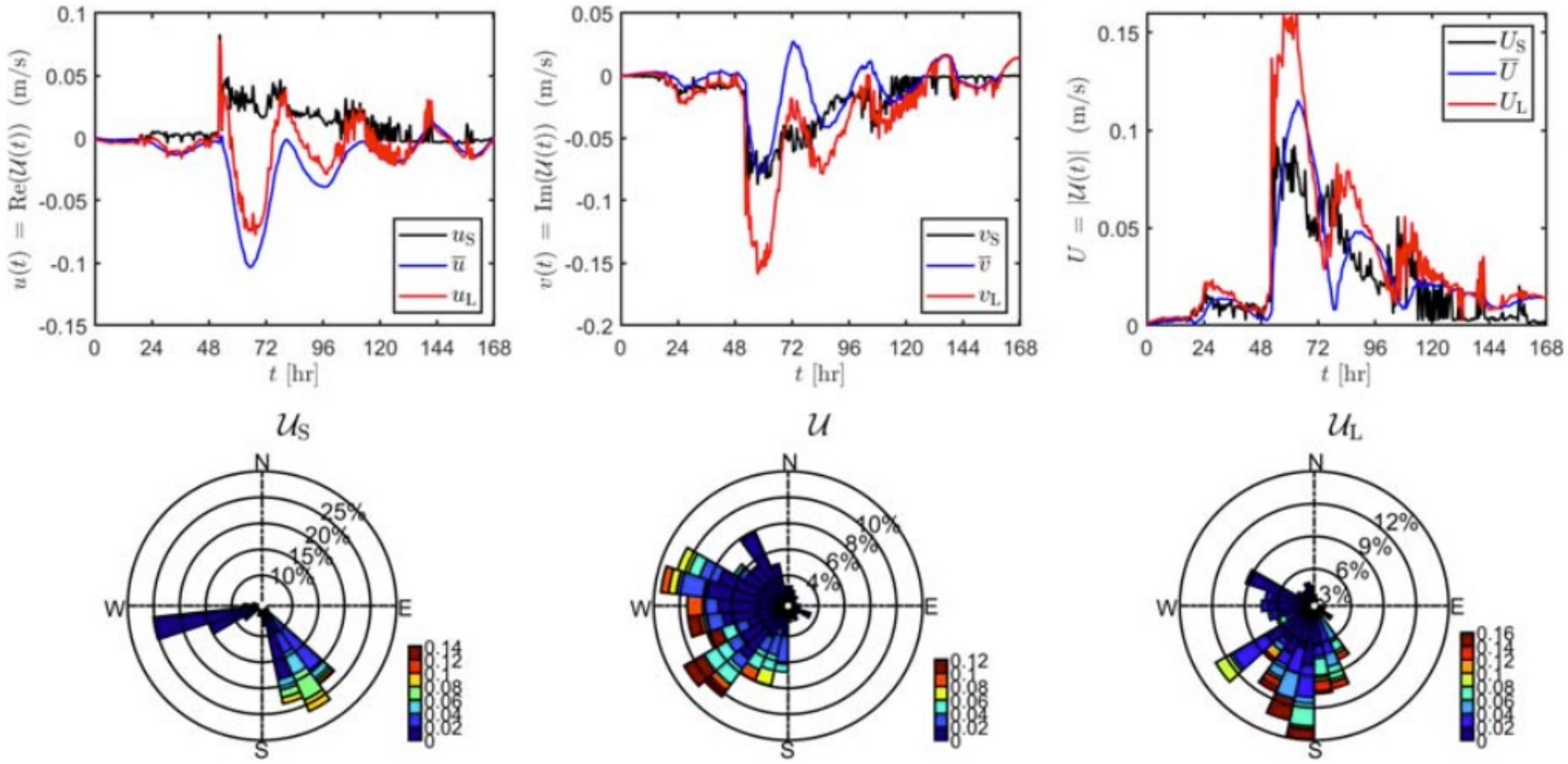

Figure 3. Top: time series (14 May 2000 15:41 to 22 May 2000 09:41 UTC) of wave-induced velocities computed from buoy data from San Nicolas Island (33.22° N, 119.88° W), with colors as in Figure 2. Bottom: corresponding wave roses, as in Figure 2.

4. Buoy data: displacements

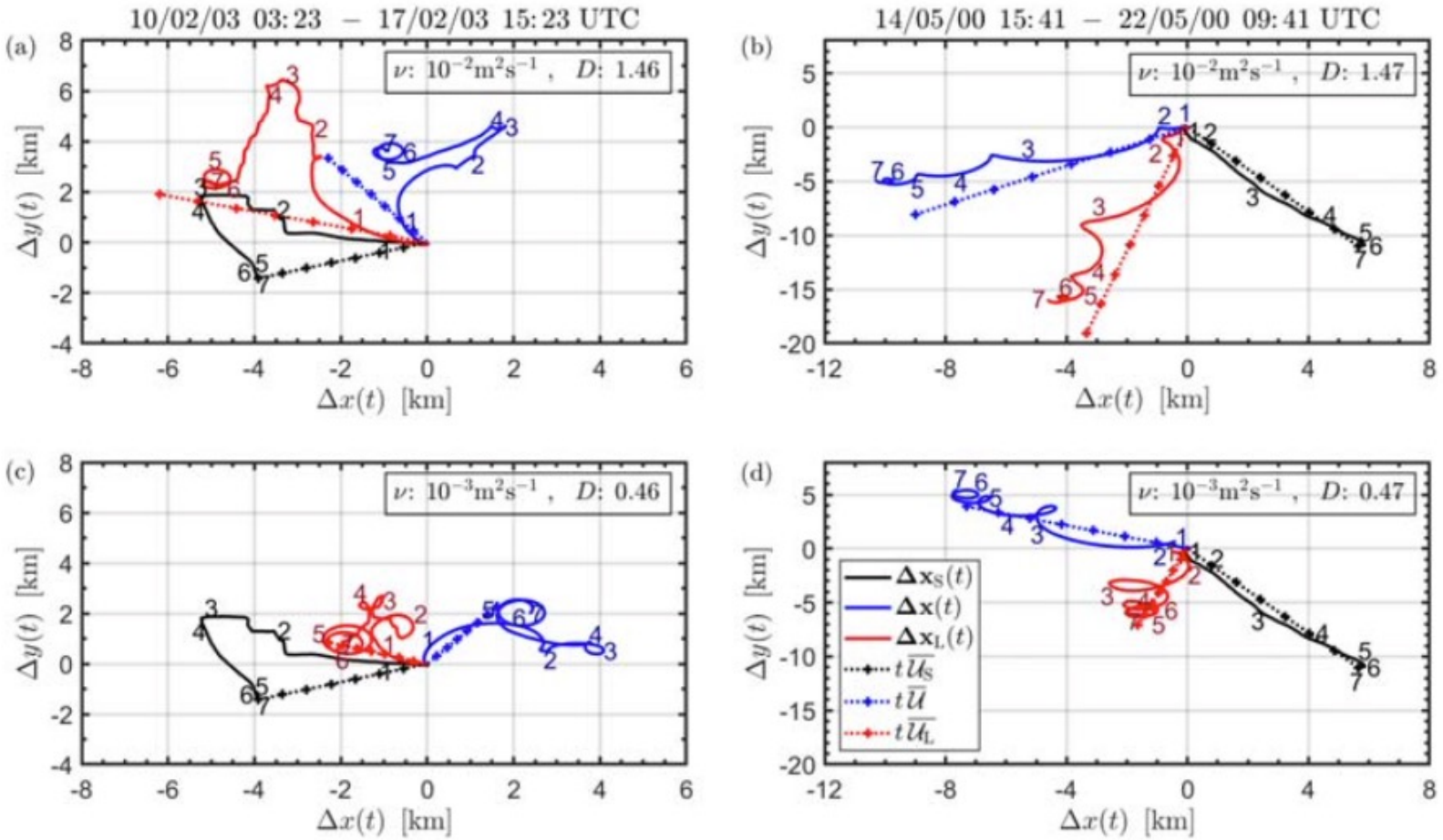

Figure 4. Particle paths at the surface ($z = 0$) computed for the San Nicolas Island buoy using our Ekman-Stokes convolution kernel. Columns: two different time samples. Rows: different values of turbulent viscosity. Paths shown are obtained using the Stokes drift (black), Eulerian-mean velocity, (blue) and Lagrangian-mean velocity (red). Dashed lines ignore time dependence of the Stokes drift and show the steady response to the average of the Stokes drift over the periods considered. All paths begin at $(\Delta x, \Delta y) = (0, 0)$. Numbers beside each line denote the number of days elapsed.

5. Ocean Parcels simulations (work in progress)

- We follow Onink et al. (2019) / Delandmeter & van Sebille (2019), adding the Ekman-Stokes flow.

- Lagrangian particles:

$$\boldsymbol{x}(t+\delta t) = \boldsymbol{x}(t) + \int_t^{t+\delta t} \boldsymbol{u}(\boldsymbol{x}(\tau), \tau) \mathrm{d}\tau,$$

- Current fields:

$$\boldsymbol{u} = \begin{cases} \boldsymbol{u}_{\mathrm{nwd}} = \boldsymbol{u}_{\mathrm{ek}} + \boldsymbol{u}_{\mathrm{geo}} & \text{Non-wave-driven (NWD) currents ,} \\ \boldsymbol{u}_{\mathrm{nwd}} + \boldsymbol{u}_{\mathrm{s}} & \text{NWD currents + Stokes drift,} \\ \boldsymbol{u}_{\mathrm{nwd}} + \boldsymbol{u}_{\mathrm{s}} + \boldsymbol{u}_{\mathrm{wde}} & \text{NWD currents + Stokes drift + wave-driven Eulerian current,} \end{cases}$$

Wave-driven Eulerian current = Ekman-Stokes flow

5. Ocean Parcels simulations

Variable	Data set	Spatial resolution	Temporal resolution	Source
Geostrophic currents	GlobCurrent v3 Geostrophic Currents	0.25°	24 hr	Rio et al. (2014)
Ekman currents	GlobCurrent v3 Ekman Hs Currents	0.25°	3 hr	Rio et al. (2014)
Total currents	GlobCurrent v3 Total Hs Currents	0.25°	3 hr	Rio et al. (2014)
Stokes drift	WaveWatch III Surface Stokes Drift	0.5°	3 hr	Ardhuin et al. (2009)
Peak frequency	WaveWatch III f_p	0.5°	3 hr	Tolman et al. (2009)
Significant wave height	WaveWatch III H_s	0.5°	3 hr	Tolman et al. (2009)
Surface wind stress	NOAA blended surface wind stress	0.25°	6 hr	Zhang et al. (2006)

5. Ocean Parcels simulations: turbulent viscosity

- Approach 1: constant turbulent value $\nu = 1.0\times10^{-2}\ m^2s^{-1}$ (Huang, 1979).
  - Problem: leads to a great deal of boundary layer streaming near the equator ($f = 0$).
  - Solution: linear reduction of viscosity to molecular value with latitude between $\pm 20°$.

- Approach 2: Mellor-Yamada 2.5 level turbulence model (we also apply the near-equator reduction).

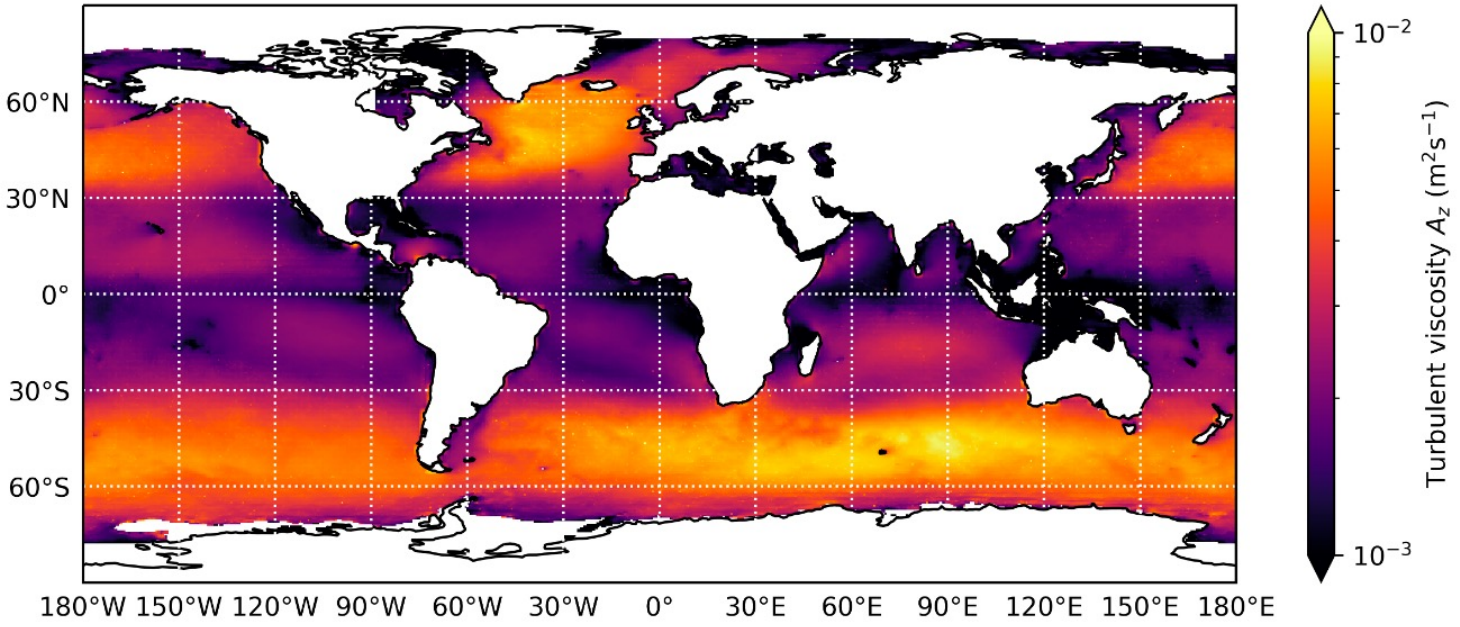

5. Ocean Parcels simulations: mean current fields

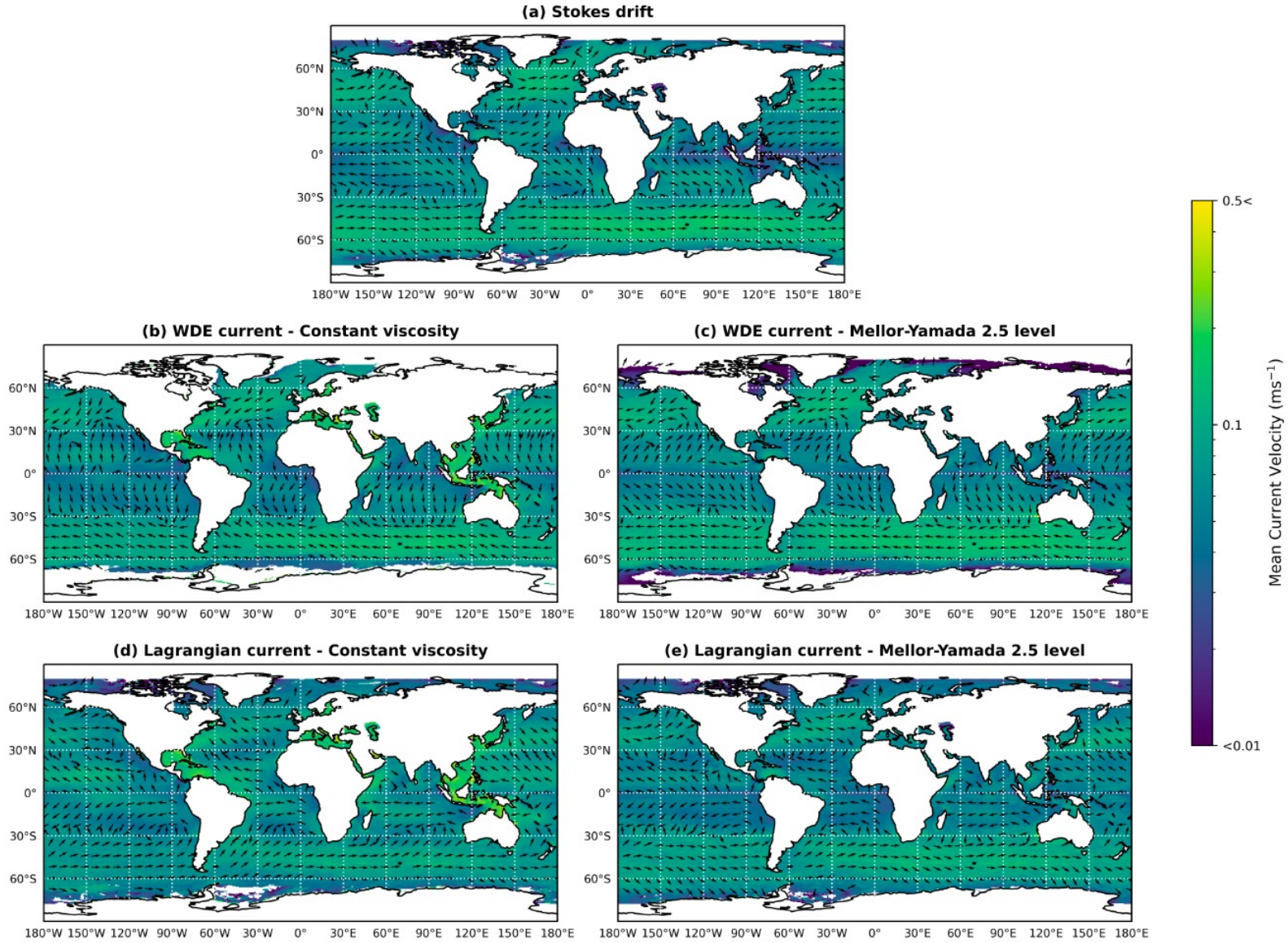

Wave-driven gyres in subtropics: reduce 'dispersive' effect of Stokes drift.

Less deflection and more 'anti-Stokes' flow at high latitudes.

Deflection away from poles flow at high latitudes.

5. Ocean Parcels simulations: final particle density

Onink et al. (2019): Stokes drift 'disperses' away from gyres.

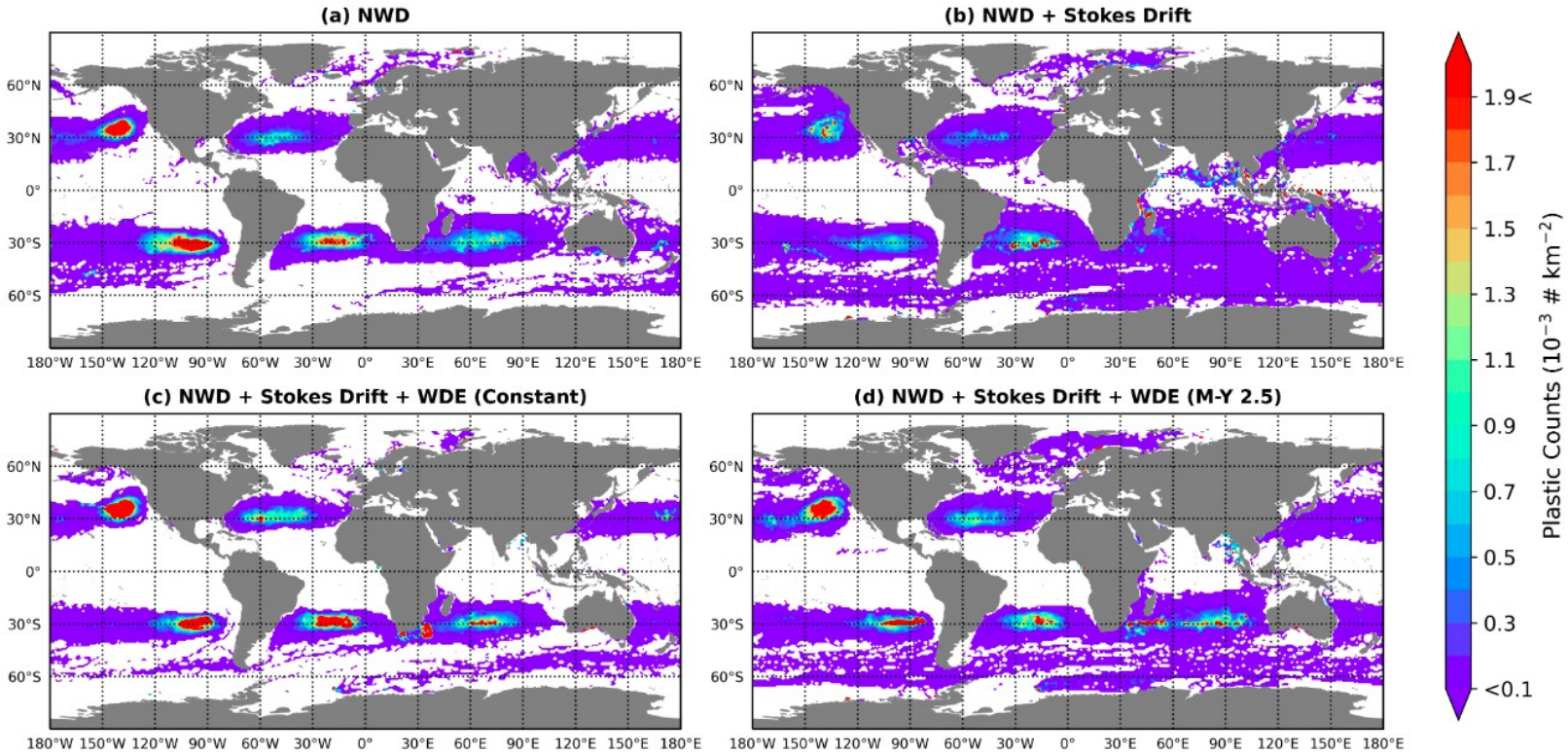

Figure 5. The average particle density for the final year of the global Lagrangian simulations with the virtual particles advected by: NWD currents (a), NWD currents + Stokes drift (b), NWD + Stokes drift + wave-driven Eulerian currents (WDE) (c and d). Simulations are from 01-01-2002 to 31-12-2014 from an initial uniform $1° \times 1°$ distribution of particles.

5. Ocean Parcels simulations: inter-basin connectivity

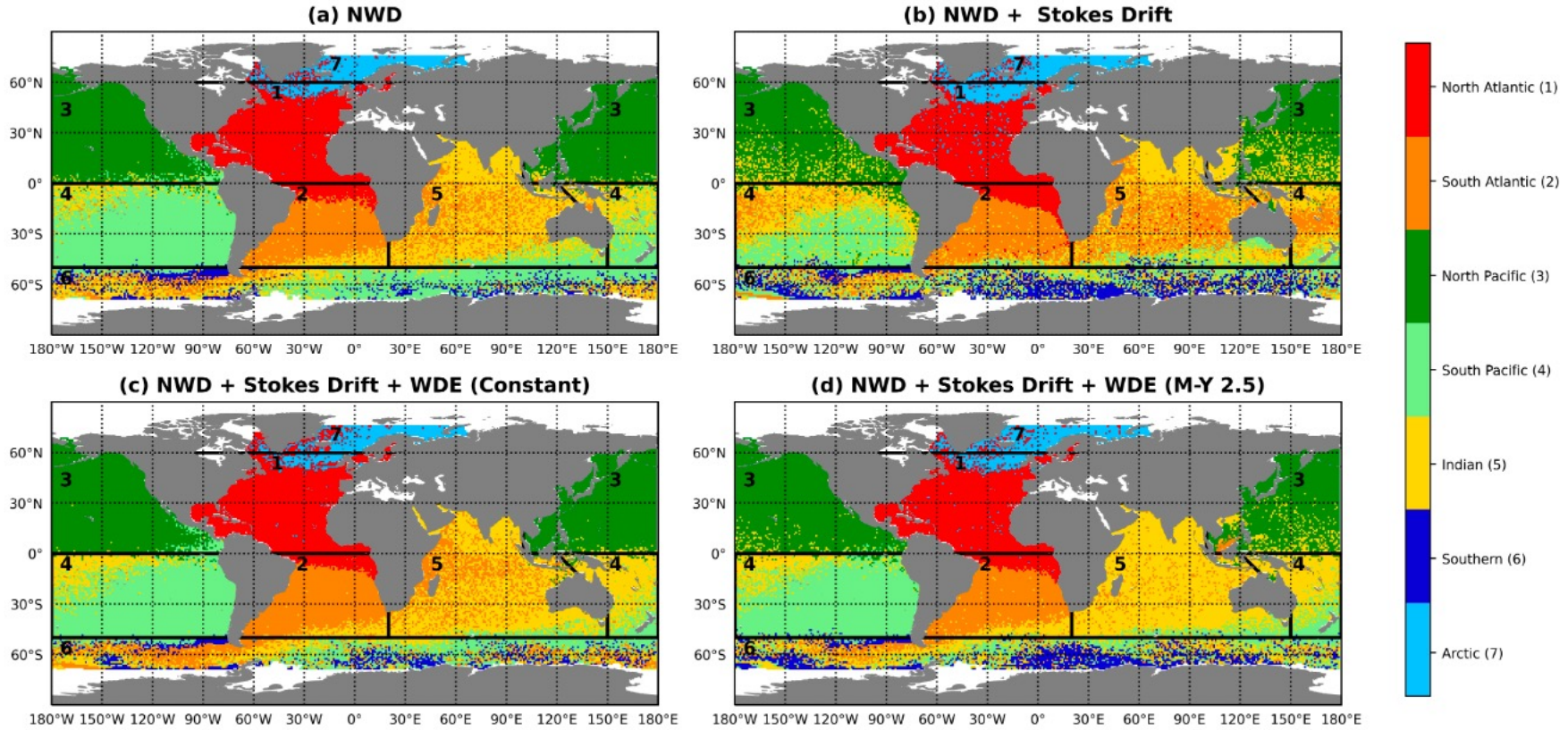

Figure 6. Inter-basin connectivity of particles for the 4 Lagrangian simulation scenarios. Particles are shown at their initial position and are colored according to their final position at the end of the simulation.

5. Ocean Parcels simulations: inter-basin connectivity

	North Atlantic				South Atlantic				North Pacific				South Pacific			
Basin of origin	**N**	**N+S**	**N+S+E1**	**N+S+E2**	**N**	**N+S**	**N+S+E1**	**N+S+E2**	**N**	**N+S**	**N+S+E1**	**N+S+E2**	**N**	**N+S**	**N+S+E1**	**N+S+E2**
North Atlantic	83.5%	77.2%	82.3%	82.8%	-	-	-	-	-	-	-	-	-	-	-	-
South Atlantic	12.5%	17.1%	11.1%	12.5%	49.1%	33.6%	43.2%	62.2%	-	-	-	-	0.1%	2.2%	-	0.3%
North Pacific	-	-	-	-	0.3%	0.2%	-	1.9%	97.3%	92.5%	96.6%	96%	1.9%	-	2.3%	0.5%
South Pacific	-	-	-	-	1.6%	17.0%	0.7%	0.5%	2.1%	6.2%	2.1%	2.9%	57.0%	45.8%	61.7%	65.6%
Indian	-	1.4%	-	-	31.2%	37.7%	29.4%	12%	0.6%	1.2%	1.3%	1.1%	7.0%	11.5%	3.8%	6.2%
Southern	-	0.3%	-	-	17.8%	11.6%	26.7%	23.4%	-	0.2%	-	-	33.9%	40.6%	32.2 %	27.3%
Arctic	3.9%	4.0%	6.6%	4.7%	-	-	-	-	-	-	-	-	-	-	-	-
Total particles	4289	4211	4367	4213	4628	6174	5616	3582	7452	6706	7592	7199	9379	5439	7468	7115

	Indian				Southern				Arctic			
Basin of origin	**N**	**N+S**	**N+S+E1**	**N+S+E2**	**N**	**N+S**	**N+S+E1**	**N+S+E2**	**N**	**N+S**	**N+S+E1**	**N+S+E2**
North Atlantic	-	-	-	-	-	-	-	-	29.7%	44.1%	32.0%	35.1%
South Atlantic	5.5%	3.3%	3.7%	4.3%	-	0.3%	-	0.3%	-	-	-	0.2%
North Pacific	1.8%	16.1%	0.9%	5.8%	-	-	-	-	-	-	-	-
South Pacific	16.0%	31.9%	24.4%	18.5%	0.9%	1.7%	0.4%	1.7%	-	-	-	-
Indian	54.8%	33.1%	50.7%	52.1%	0.3%	2.3%	0.2%	0.7%	-	0.1%	-	-
Southern	21.9%	15.5%	19.8%	19.3%	98.9%	95.6%	99.4%	97.3%	-	-	-	-
Arctic	-	-	-	-	-	-	-	-	70.3%	55.8%	68.0%	64.7%
Total particles	6927	8445	7711	9552	1159	2524	1246	2104	1276	1611	1145	1345

Table 4. Global statistics describing the composition of microplastics in a given ocean basin at the end of the 14-year simulation, given the basin of origin of the particles. N = NWD currents, S = Stokes drift, E1 = Wave-driven Eulerian current (Constant viscosity model), E2 = Wave-driven Eulerian current (Mellor-Yamada viscosity model).

5. Ocean Parcels simulations: inter-basin connectivity

Onink et al. (2019): more cross-equator transport due to Stokes drift

	North Atlantic				South Atlantic				North Pacific				South Pacific			
Basin of origin	**N**	**N+S**	**N+S+E1**	**N+S+E2**	**N**	**N+S**	**N+S+E1**	**N+S+E2**	**N**	**N+S**	**N+S+E1**	**N+S+E2**	**N**	**N+S**	**N+S+E1**	**N+S+E2**
North Atlantic	83.5%	77.2%	82.3%	82.8%	-	-	-	-	-	-	-	-	-	-	-	-
South Atlantic	12.5%	17.1%	11.1%	12.5%	49.1%	33.6%	43.2%	62.2%	-	-	-	-	0.1%	2.2%	-	0.3%
North Pacific	-	-	-	-	0.3%	0.2%	-	1.9%	97.3%	92.5%	96.6%	96%	1.9%	-	2.3%	0.5%
South Pacific	-	-	-	-	1.6%	17.0%	0.7%	0.5%	2.1%	6.2%	2.1%	2.9%	57.0%	45.8%	61.7%	65.6%
Indian	-	1.4%	-	-	31.2%	37.7%	29.4%	12%	0.6%	1.2%	1.3%	1.1%	7.0%	11.5%	3.8%	6.2%
Southern	-	0.3%	-	-	17.8%	11.6%	26.7%	23.4%	-	0.2%	-	-	33.9%	40.6%	32.2 %	27.3%
Arctic	3.9%	4.0%	6.6%	4.7%	-	-	-	-	-	-	-	-	-	-	-	-
Total particles	4289	4211	4367	4213	4628	6174	5616	3582	7452	6706	7592	7199	9379	5439	7468	7115

	Indian				Southern				Arctic			
Basin of origin	**N**	**N+S**	**N+S+E1**	**N+S+E2**	**N**	**N+S**	**N+S+E1**	**N+S+E2**	**N**	**N+S**	**N+S+E1**	**N+S+E2**
North Atlantic	-	-	-	-	-	-	-	-	29.7%	44.1%	32.0%	35.1%
South Atlantic	5.5%	3.3%	3.7%	4.3%	-	0.3%	-	0.3%			-	0.2%
North Pacific	1.8%	16.1%	0.9%	5.8%	-	-	-	-	-	-	-	-
South Pacific	16.0%	31.9%	24.4%	18.5%	0.9%	1.7%	0.4%	1.7%	-	-	-	-
Indian	54.8%	33.1%	50.7%	52.1%	0.3%	2.3%	0.2%	0.7%	-	0.1%	-	-
Southern	21.9%	15.5%	19.8%	19.3%	98.9%	95.6%	99.4%	97.3%	-	-	-	-
Arctic	-	-	-	-	-	-	-	-	70.3%	55.8%	68.0%	64.7%
Total particles	6927	8445	7711	9552	1159	2524	1246	2104	1276	1611	1145	1345

Table 4. Global statistics describing the composition of microplastics in a given ocean basin at the end of the 14-year simulation, given the basin of origin of the particles. N = NWD currents, S = Stokes drift, E1 = Wave-driven Eulerian current (Constant viscosity model), E2 = Wave-driven Eulerian current (Mellor-Yamada viscosity model).

Onink et al. (2019): Indian ocean better connected due to Stokes drift

Onink et al. (2019): more transport due to the poles due to Stokes drift

5. Ocean Parcels simulations: inter-basin connectivity

	North Atlantic				South Atlantic				North Pacific				South Pacific			
Basin of origin	**N**	**N+S**	**N+S+E1**	**N+S+E2**	**N**	**N+S**	**N+S+E1**	**N+S+E2**	**N**	**N+S**	**N+S+E1**	**N+S+E2**	**N**	**N+S**	**N+S+E1**	**N+S+E2**
North Atlantic	83.5%	77.2%	82.3%	82.8%	-	-	-	-	-	-	-	-	-	-	-	-
South Atlantic	12.5%	17.1%	11.1%	12.5%	49.1%	33.6%	43.2%	62.2%	-	-	-	-	0.1%	2.2%	-	0.3%
North Pacific	-	-	-	-	0.3%	0.2%	-	1.9%	97.3%	92.5%	96.6%	96%	1.9%	-	2.3%	0.5%
South Pacific	-	-	-	-	1.6%	17.0%	0.7%	0.5%	2.1%	6.2%	2.1%	2.9%	57.0%	45.8%	61.7%	65.6%
Indian	-	1.4%	-	-	31.2%	37.7%	29.4%	12%	0.6%	1.2%	1.3%	1.1%	7.0%	11.5%	3.8%	6.2%
Southern	-	0.3%	-	-	17.8%	11.6%	26.7%	23.4%	-	0.2%	-	-	33.9%	40.6%	32.2 %	27.3%
Arctic	3.9%	4.0%	6.6%	4.7%	-	-	-	-	-	-	-	-	-	-	-	-
Total particles	4289	4211	4367	4213	4628	6174	5616	3582	7452	6706	7592	7199	9379	5439	7468	7115

	Indian				Southern				Arctic			
Basin of origin	**N**	**N+S**	**N+S+E1**	**N+S+E2**	**N**	**N+S**	**N+S+E1**	**N+S+E2**	**N**	**N+S**	**N+S+E1**	**N+S+E2**
North Atlantic	-	-	-	-	-	-	-	-	29.7%	44.1%	32.0%	35.1%
South Atlantic	5.5%	3.3%	3.7%	4.3%	-	0.3%	-	0.3%	-	-	-	0.2%
North Pacific	1.8%	16.1%	0.9%	5.8%	-	-	-	-	-	-	-	-
South Pacific	16.0%	31.9%	24.4%	18.5%	0.9%	1.7%	0.4%	1.7%	-	-	-	-
Indian	54.8%	33.1%	50.7%	52.1%	0.3%	2.3%	0.2%	0.7%	-	0.1%	-	-
Southern	21.9%	15.5%	19.8%	19.3%	98.9%	95.6%	99.4%	97.3%	-	-	-	-
Arctic	-	-	-	-	-	-	-	-	70.3%	55.8%	68.0%	64.7%
Total particles	6927	8445	7711	9552	1159	2524	1246	2104	1276	1611	1145	1345

Table 4. Global statistics describing the composition of microplastics in a given ocean basin at the end of the 14-year simulation, given the basin of origin of the particles. N = NWD currents, S = Stokes drift, E1 = Wave-driven Eulerian current (Constant viscosity model), E2 = Wave-driven Eulerian current (Mellor-Yamada viscosity model).

6. Validation with field data (thanks to Lavender Law, Onink, van Sebille)

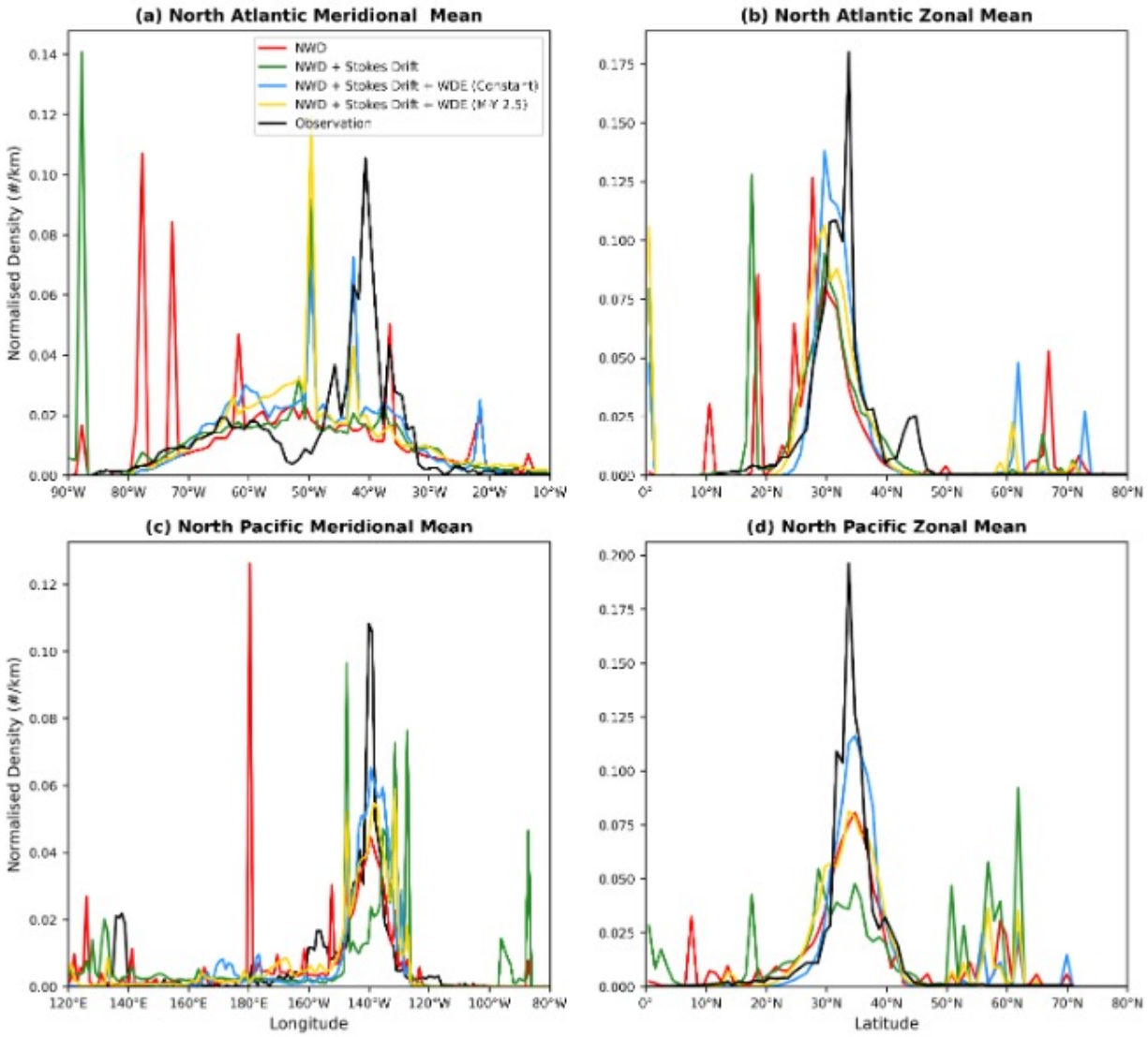

7. Conclusions

- Surface waves can drive Ekman-like flows, with the additional effect of the Coriolis-Stokes forcing.
- Using a simple convolution integral, the leading-order Ekman-Stokes flow is easily calculated.
- The Ekman-Stokes can significantly affect the drift of floating objects.
- The Ekman-Stokes flow (at the surface) is sensitive to the value of viscosity.
- The Ekman-Stokes flow opposes the dispersive behaviour of Stokes drift: cross-Equator+polar transport reduced.
- The Ekman-Stokes perhaps improves somewhat agreement between models and observational data.

Further work:

- Broad-banded spectra
- Alternate depth profiles for eddy viscosity
- Spatial variation
- Stratification, background flow, instabilities

Literature

Higgins, C., J. Vanneste & T.S. van den Bremer (2020) Unsteady Ekman-Stokes dynamics: implications for surface wave-induced drift of floating marine litter. Geophysical Research Letters. 47, e2020GL089189.

Cunningham, H.J., C. Higgins & T.S. van den Bremer (under review) The role of the unsteady surface wave-driven Ekman-Stokes flow in the accumulation of floating marine litter.